DESY Summer School Project Report

14th September 2007

Address:

Gohar Tsakanova,

Yerevan State University,

Yerevan,

Alek Manoogyan 1,

Republic of Armenia

Email: tsakanova@yahoo.com

Title: "Characterization of protein behavior in crystallization experiments"

Supervisor: Dr. Matthew Groves

Abstract:

X-ray protein diffraction experiments remain the dominant form of structural biology in modern science, due to the application of high throughput techniques and the availability of synchrotron radiation. The advances in modern X-ray crystallography have led directly to the current population of the protein structural database (45,744 to date). However, the production of protein crystals remains a bottleneck in the field and further efforts are needed to understand the chemical and physical laws that govern protein crystallization. In this study we have used a non-invasive fluorescent dye (1,8-anilinonaphthalene sulphonate) to study the effects of varying crystallization conditions upon the solution state of lysozyme. In our initial experiments the saturation state of lysozyme is clearly available for the first time. Previously, visible light illumination could make no distinction between these conditions.

Table of Contents

1.0 General Introduction

The general method of protein structure determination is protein crystallization with subsequent X-Ray diffraction. The vast majority of the 45,774 structures deposited at the PDB (www.rcsb.org) have been determined using X-ray crystallography. Crystallography allows scientists, through the study of protein crystals, to determine the three-dimensional molecular structures of proteins, other large molecular assemblies and viruses. The ability to know the atomic molecular structure of biological macromolecules has revolutionized the study of their functions in many fields of biology:

Structural biology – The study of the fundamental molecules of life has been made possible through the advances in protein crystallography. The atomic resolution information has elucidate a vast number of biological processes and continues to be high impact research. The examples are far too numerous and diverse to list here.

Drug design - The design of drugs is related to this, and involves designing a molecule that can exactly fit into a binding site of a macromolecule and block its function in the disease pathway (e.g. Kroemer, R.T. "Structure-based drug design: docking and scoring.Curr" *Protein Pept Sci*. (2007), **8(4)**:312-28.).

Bioseparations - Bioseparations refers to the downstream processing of the products of fermentation. Typically the desired product of the fermentation process is a protein (e.g. insulin), which then needs to be separated from the biomass. Crystallization is one of the commonly employed techniques for separating the protein. It has the advantage of being a benign separations process, that is, it does not cause the protein to unfold and lose its activity. The issues here are better prediction and control of the crystallization process to facilitate improved design of crystallization units. (e.g. Malek K. "Solute transport in orthorhombic lysozyme crystals: a molecular simulation study" *Biotechnol Lett.* (2007), **7(20).**

Controlled drug delivery - Most drugs are cleared by the body rapidly following administration, making it difficult to achieve a constant desired level over a period of time. When the drug is a protein (such as insulin or alpha-interferon), administering the

drug in the crystalline form shows promise of achieving such controlled delivery and clinical trials are already underway to test it. The challenge here is to produce crystals of relatively uniform sizes so that the dosage can be prescribed correctly. (e.g. Villari V, Micali N. "Light scattering as spectroscopic tool for the study of disperse systems useful in pharmaceutical sciences" *J Pharm Sci.* 2007 9(5).

However, the initial requirement is for crystals that diffract well and the growth of these samples remains the major bottleneck in structural biology today. Once a suitable crystal has been grown it is mounted in a cryo-protective buffer and placed in an X-ray beam from either a laboratory or a synchrotron source. Much of the data collection steps have been automated, leading to an efficient protocol for structural biology that does not require expert training (e.g. Panjikar S, Parthasarathy V, Lamzin V.S., Weiss M.S., Tucker P.A. "Auto-Rickshaw: an automated crystal structure determination platform as an efficient tool for the validation of an X-ray diffraction experiment" *Acta Crystallogr D Biol Crystallogr.* 2005 Apr;61(Pt 4):449-57).

1.1 Protein Crystal Formation

Protein crystals appear when the protein solution becomes saturated. The saturation of protein solution depends on the solubility of the proteins. The solubility of proteins can be represented in phase diagrams, which plot the solubility curve of a protein (Fig.1.). A so-called meta-stable state occurs when the rate of loss and gain of both the solid and solution phases of the protein are equal, and the system is in equilibrium.

Salting-out is seen on the right hand side of Fig. 1 where there is a reduction in protein solubility as the concentration of salt increases. Salting-in is seen on the left hand side of Fig 1. where there is an increase in protein solubility as the concentration of salt increases.

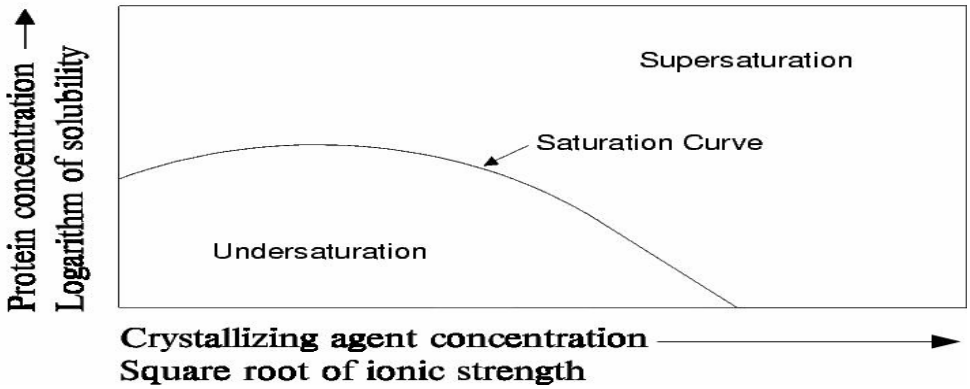

Fig.1. Phase Diagram for a typical protein: The horizontal axis shows the Parameter being varied (usually precipitant concentration); and the vertical axis shows the protein concentration.
(*http://www-structmed.cimr.cam.ac.uk/Course/Crystals/Theory/phases.html).*

In the crystal growth process there is a general interest of how the protein becomes supersaturated and why the protein does not immediately precipitate or crystallize as soon as saturation is achieved. This is because the protein has to overcome an energy barrier to crystallization analogous to that for conventional chemical reactions (Fig.2.)

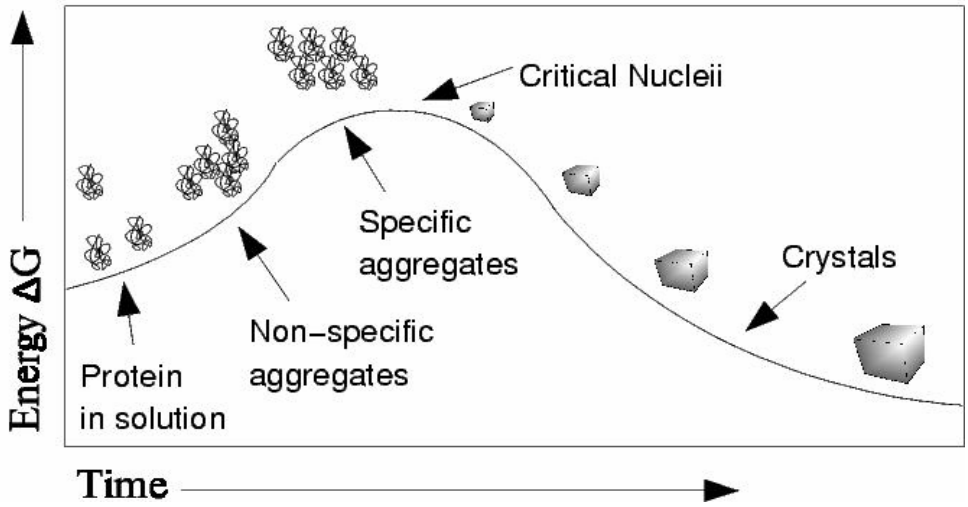

Fig. 2. Energy Diagram for Crystallization: The critical nucleus corresponds to the higher energy intermediate. The higher the energy barrier, the slower the rate of nucleation.
(*http://www-structmed.cimr.cam.ac.uk/Course/Crystals/Theory/phases.html).*

The increase in supersaturation leads to the increasing of the probability of nucleation (Fig.3.). The more supersaturated the protein solution, the greater the likelihood that a critical nucleus will form, the smaller the nucleus needed to induce crystal formation. This can be represented on a phase diagram by dividing the supersaturated zone into regions of increasing probability of nucleation and precipitation.

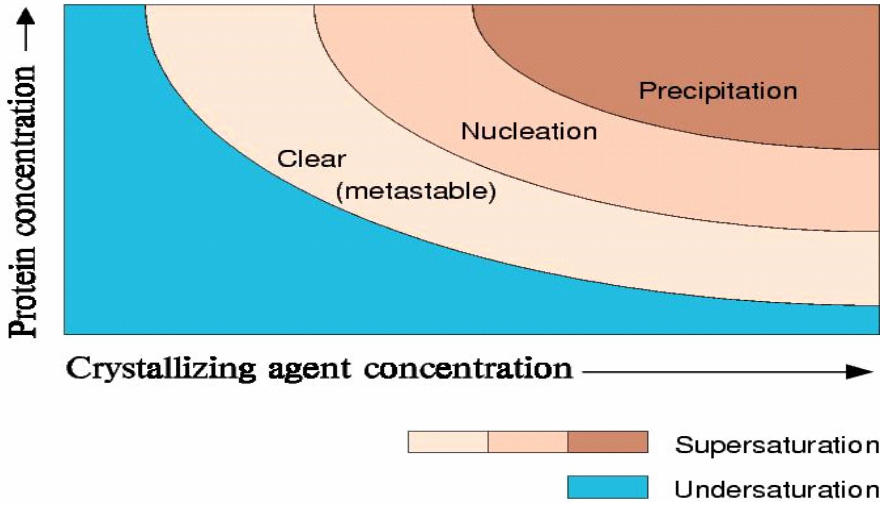

Fig.3. Phase Diagram showing zones for crystal nucleation, growth and precipitation.
(http://www-structmed.cimr.cam.ac.uk/Course/Crystals/Theory/phases.html).

1.2 Crystallization Experiments

There are a number of available methods for protein crystallization:

- Vapor diffusion
    - Hanging drop
    - Sitting drop
    - Sandwich drop
- Batch crystallization
- Dialysis

1.2.1 Vapour Diffusion

In the vapour diffusion technique (e.g. MCPHERSOX, A. "Preparation and Analysis of Protein Crystals" New York: Wiley. (1982)) the fluids are not in direct contact, but crystallization occurs as the fluids evaporate. In a vapour diffusion experiment, small volumes of precipitant and protein mixed together and the drop equilibrated against a larger reservoir of solution containing precipitant or another dehydrating agent. Initially, the droplet of protein solution contains an insufficient concentration of precipitant for crystallization, but as water vaporizes from the drop and transfers to the reservoir, the precipitant concentration increases to a level optimal for crystallization (Fig.4.). Since the system is in equilibrium, these optimum conditions are maintained until the crystallization is complete. After sealing, the solution equilibrates to achieve supersaturating concentrations of protein and thereby induce crystallization in the drop.

The vapor diffusion method can be implemented in three ways, hanging drop, sitting drop and, so-called sandwich drop. It is important to mention that this three methods require a closed system, that is, the system must be sealed off from the outside using an airtight container or high-vacuum grease between glass surfaces (Fig.4.).

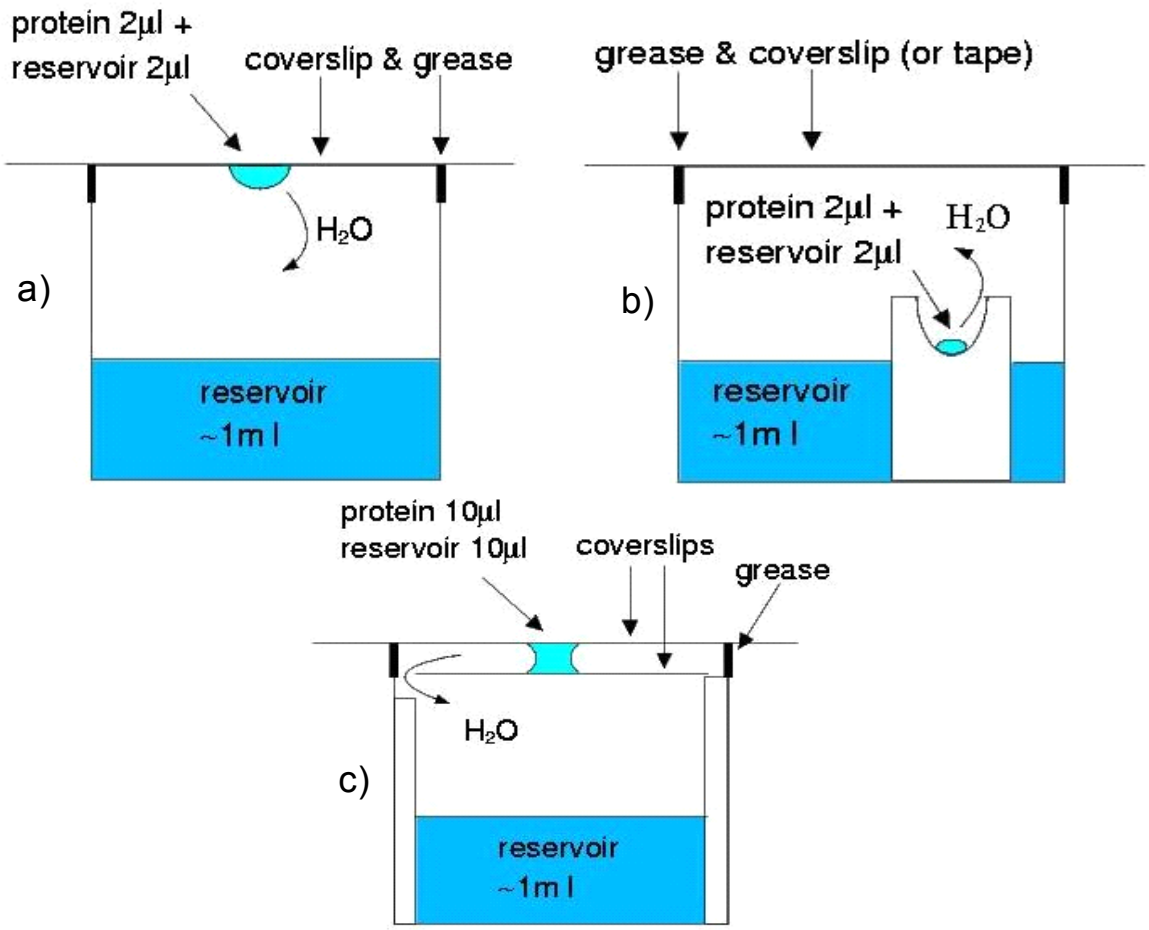

Fig.4. a) Hanging drop vapour diffusion; b) sitting drop vapor diffusion; c) sandwich drop vapour diffusion.
(http://www-structmed.cimr.cam.ac.uk/Course/Crystals/Theory/methods.html).

The hanging drop method differs from the sitting drop method in the vertical orientation of the protein solution drop within the system (Fig.4.a). In the sitting drop vapor diffusion method, the protein drop sits on a pedestal above the reservoir solution (Fig.4.b), as opposed to hanging drop. In the sandwich drop vapor diffusion method, the protein drop places between two glass shelves (Fig.4.c).

1.2.2 Batch Crystallization

In batch crystallization the precipitant and protein are mixed directly under oil, and the precipitant and protein concentration stay the same (Fig.5).

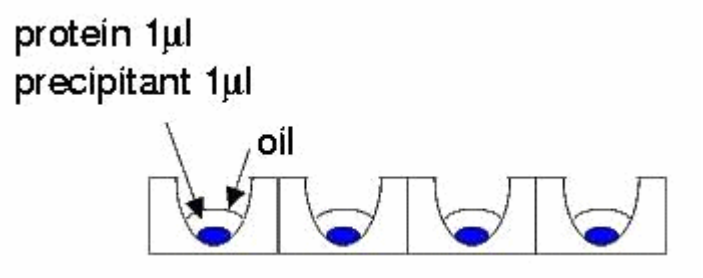

Fig. 5. Batch experiment.
(http://wwwstructmed.cimr.cam.ac.uk/Course/Crystals/Theory/methods.html)

1.2.3 Dialysis

In a dialysis crystallization experiment, protein is equilibrated against a larger volume of precipitant through a dialysis membrane (Fig.6). In this case the concentration of the protein is constant.

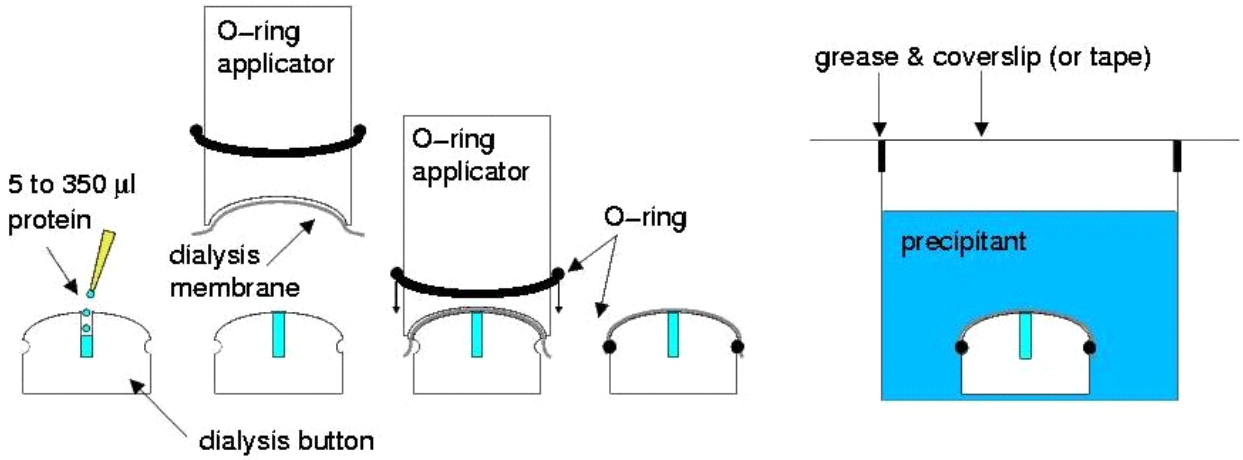

Fig. 6. Dialysis experiment.
(http://www-structmed.cimr.cam.ac.uk/Course/Crystals/Theory/methods.html).

1.3 Crystallization Phase Diagrams

The protein crystallization process can be explained by the phase diagrams. It is possible to create the phase diagram for the types of crystallization experiments described above.

1.3.1 Hanging drop Phase Diagrams

In a vapour diffusion experiment where equal volumes of precipitant and protein are added in the drop, both the precipitant and protein concentration will have doubled at the final equilibrium state. In Fig. 7 a vapor diffusion diagram in the case of crystals are not grown yet. However, if crystals begin to grow, the concentration of protein in solution will decrease (Fig.8).

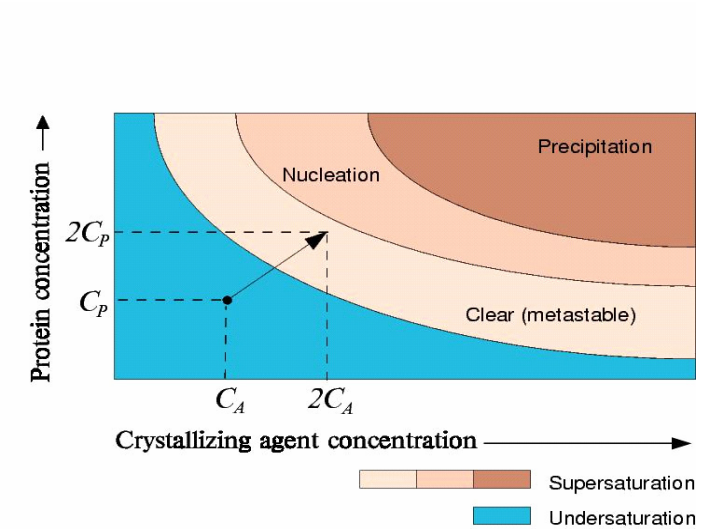

Fig. 7. Phase Diagram for vapour diffusion experiment, no crystals.
(http://www-structmed.cimr.cam.ac.uk/Course/Crystals/Theory/phase_methods.html).

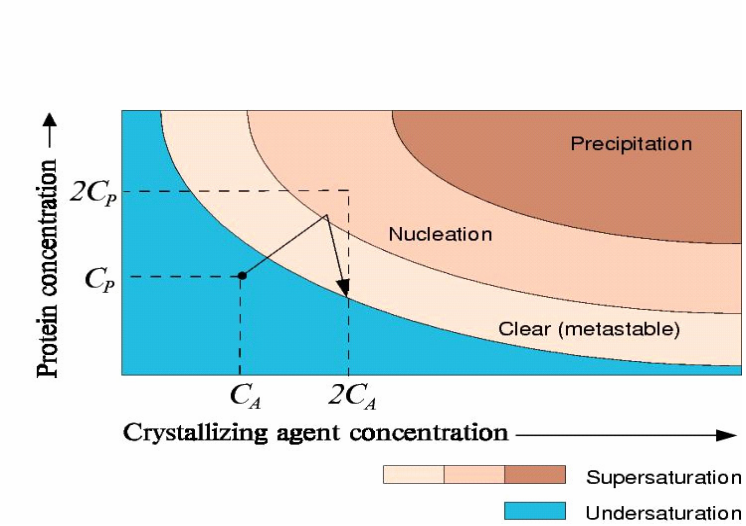

Fig. 8. Phase Diagram for vapour diffusion experiment, crystals growing.
(http://www-structmed.cimr.cam.ac.uk/Course/Crystals/Theory/phase_methods.html).

1.3.2 Batch crystallization Phase Diagrams

Figure 9 below provides the phase diagram for batch crystallization. In this type of experiment the protein concentration remains constant, as a result many more individual points in chemical space need to be tested in order to adequately sample crystallization space. In figure 9 the example is off 3 independent experiments, although many more may be required in reality.

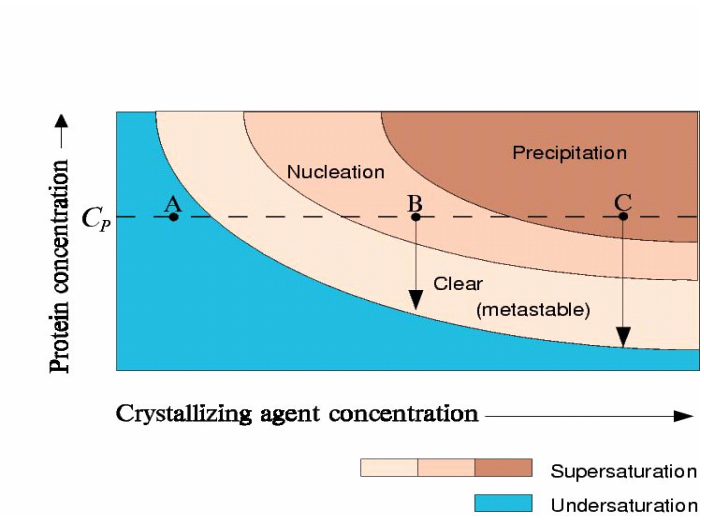

Fig.9. Phase diagram for batch crystallization: Point A - Protein stays undersaturated; point B: Protein crystallizes and the concentration of protein in solution drops to saturation; point C: Protein precipitates, but crystals may still grow.
(http://www-structmed.cimr.cam.ac.uk/Course/Crystals/Theory/phase_methods.html).

1.3.3 Dialysis Phase Diagrams

Dialysis has the advantage, that the precipitant concentration can be altered during the course of the experiment (Fig.10a). In the dialysis experiment it is also possible to increase the concentration of one precipitating agent while decreasing the concentration of another (Fig.10b). Dialysis can also be used to exploit the salting-in region of the phase diagram by forcing the protein out of solution by lowering the precipitant concentration (Fig.10c).

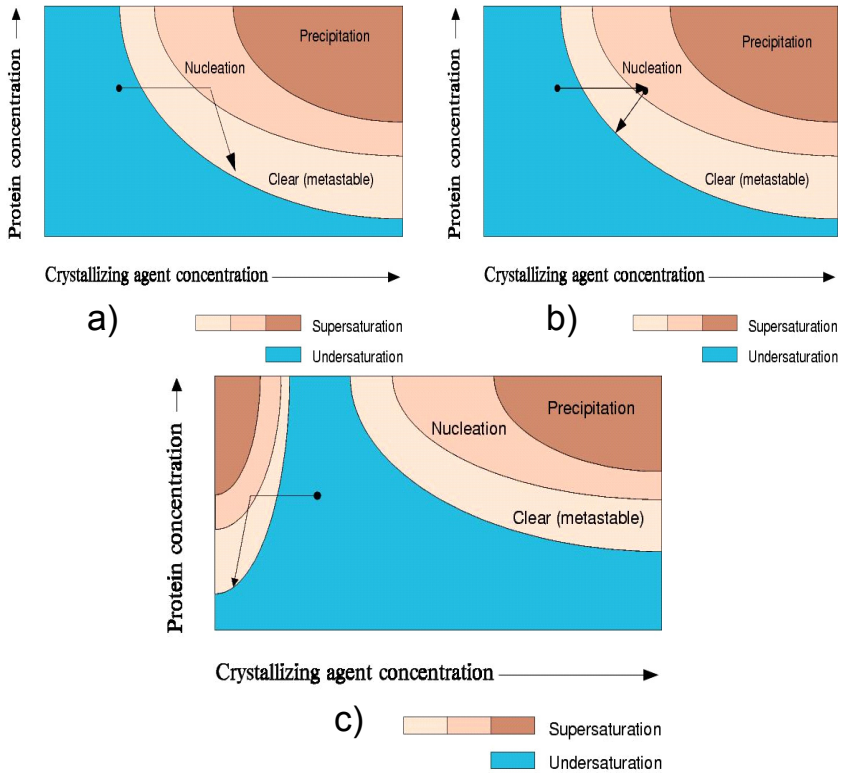

Fig. 10. Phase diagram for dialysis experiment: a) phase diagram for A salting-out dialysis experiment: In this case, the precipitant concentration increases; b) phase diagram for a dialysis experiment, changing buffers; c) phase diagram for desalting.
(http://www-structmed.cimr.cam.ac.uk/Course/Crystals/Theory/phase_methods.html).

For the crystallization experiments it is very important to know and to keep the crystallization plates in the right conditions. The important parameters of crystallization condition are protein concentration, pH, precipitant or salt concentration and temperature.

1.4 Experimental Design

As detailed above there exist a number of methods that have been used for protein crystallization. However, the determination of the protein state within the phase diagram is non-trivial - given that the protein is soluble at points in the phase diagram until after nucleation has been reached. We followed on from previous research using the non-invasive fluorescence dye 1,8-anilinonaphthalene sulphonate to study the solution state of proteins over the phase diagram.

Lysozyme was chosen as a model system as it has a large number of known crystallization states that cover a range of buffer pH's and precipitant types. The resulting crystallization experiments were visualized and analyzed under visible and fluorescent light conditions.

2. Materials and methods

2.1 Reagents

Lysozyme was dissolved in water at a concentration of 30mg/ml as determined by its absorption at 280nm. The fluorescent dye ANS (1,8-anilinonaphthalene sulphonate) was prepared at a concentration of 1.5mM as determined by its absorption at 372nm. Protein and dye solutions were mixed in order to produce a sample in which the final ANS concentrations were 0.1 mM and 0.01 mM. A control sample of undiluted lysozyme was also prepared. All other chemicals were standard laboratory grade, unless stated otherwise.

2.2 Crystallization Controls

In order to demonstrate the quality of the lysozyme, the undiluted sample was used in a standard crystallization screen around the best known conditions (1.6M NaCl, 100mM Na Acetate pH 4.6).

2.3 Crystallization in the presence of ANS

A number of different conditions were chosen under which lysozyme gives crystals. Screens were designed around these conditions such that either the buffer pH or precipitant concentration was varied. Lysozyme/dye samples were screened against these conditions using the sitting drop technique on the automated high throughput robot available at the EMBL Hamburg Outstation (Jochen Mueller-Dieckmann "The open-access high-throughput crystallization facility at EMBL Hamburg" *Acta Crystallogr D Biol Crystallogr.* 2006 D62 (1446-1452)). In total 96 well plates (3 at each ANS concentration) were produced, in which the protein and screen volumes were 300nl. The samples were allowed to incubate at room temperature for 2 weeks prior to visualization under fluorescent conditions. Visible light images were taken automatically via the integrated camera in the HTP crystallization robot. Image analysis of the crystallization images was performed using Photoshop®.

3. Results

As previously determined, the crystallization rates of lysozyme were unaffected by the concentrations of ANS used in this study, as evidenced by the total number of condition ranges (pH gradients or precipitant gradients – see supplementary information contained in GT1.xls, GT2.xls and GT3.xls) in which crystals were formed in both dye concentrations (0.1mM ANS: 13 ; 0.01mM ANS: 13).

A total of 576 images were taken under fluorescent conditions and analysis is still underway at the time of writing. The data presented below is therefore preliminary. We present below the results of analysis of only 1 condition ranges: a precipitant screen (Figs. 15-18).

3.1 Fluorescent and Visible imaging of a precipitant screen

Figure 15 below shows images of the lysozyme crystallization experiments under visible light conditions. An examination of the images shows that there is no precipitation present in any of the conditions screened. This demonstrates that this experiment did not reach the precipitation region of the phase diagram. Large crystals start to become observable in 15e and 15f. Under visible light illumination conditions no crystals are visible in any of the other conditions.

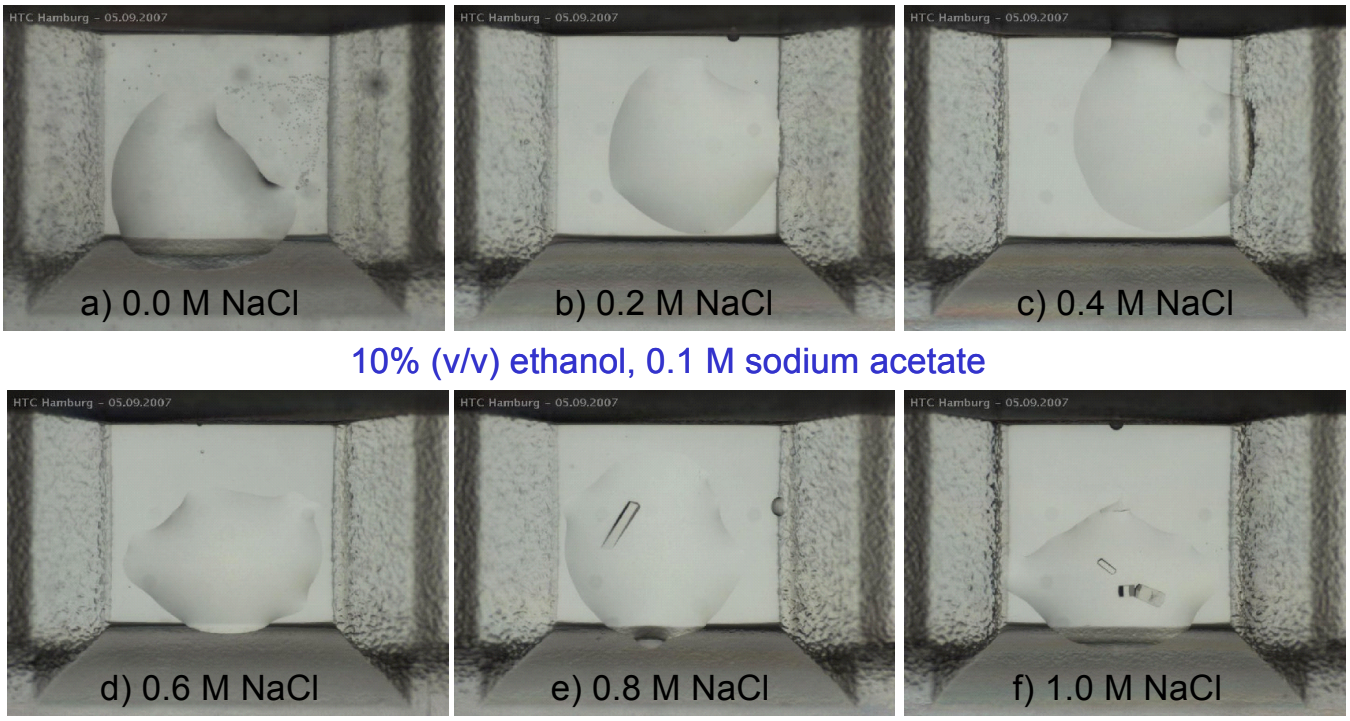

Fig.15. Lysozyme crystallization images taken under visible light conditions.

Fluorescent imaging of the same drops provides a clearer indication of the presence of crystals as demonstrated in Figure 16. Differences in the orientation of the visible and fluorescent light images are entirely due to the manual mounting of the crystallization plate on the fluorescent microscope stage. This result is in agreement with previously published research (e.g. Groves M.R. et el. "A Method for the general identification of protein crystals in crystallization experiments using a noncovalent fluorescent dye" *Acta Crystallogr D Biol Crystallogr.* 2007 D**63** (526-535).

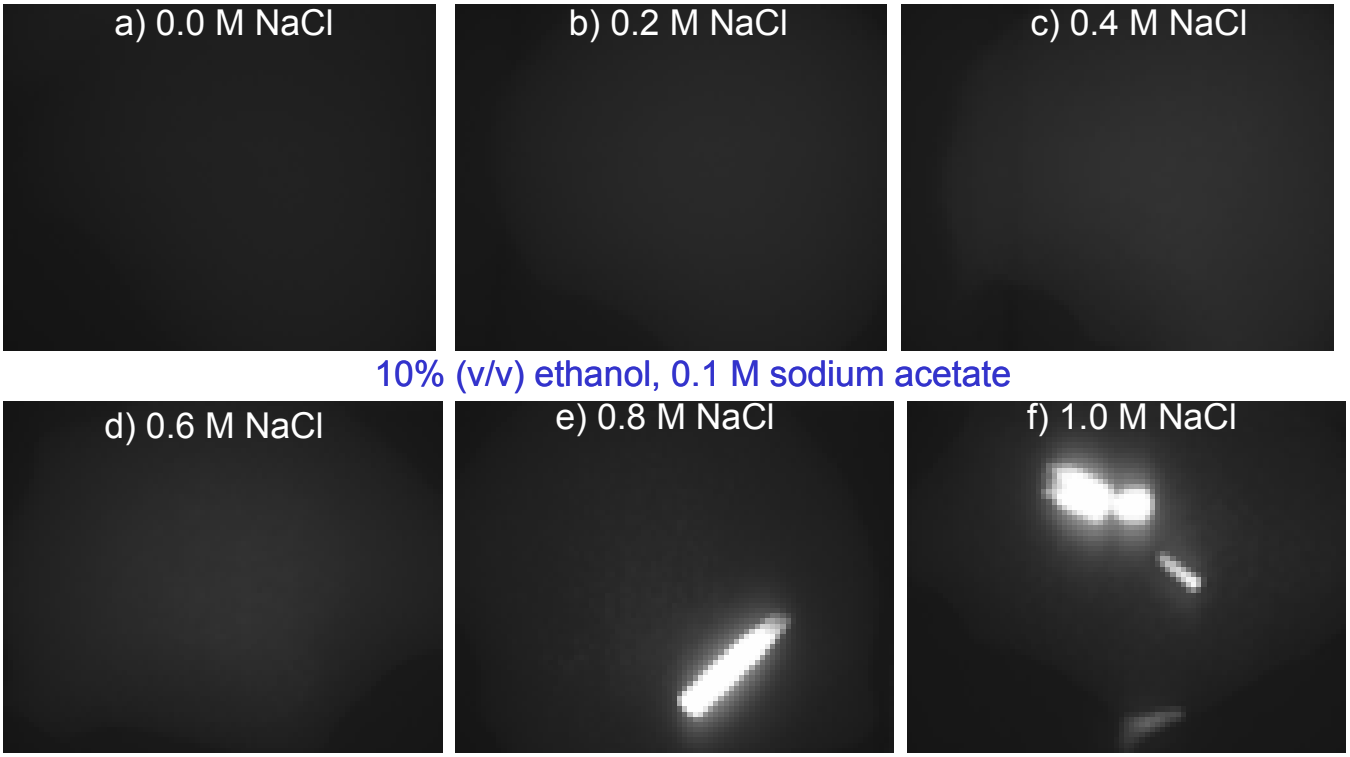

Fig. 16. Lysozyme crystallization images taken under fluorescent light conditions.

Subsequent image manipulation was then performed using Photoshop®. The intensity histograms of each image were then examined (Fig. 17). The images corresponding to those which contain crystals visible under normal illumination conditions clearly showed saturation effects (pixels with counts >256). To our surprise the analysis of the histograms of the drops that were clear under visible light (and thus indistinguishable) did not show identical intensity histograms under fluorescent visualization (Fig. 17 a)-d)). Rather a distinct change in the distribution is visible at pixel values of 50 counts. As the precipitation conditions increase there is a correlated rise in the mean value of the intensity distribution from 28.33 counts to 35.38 counts. This result we interpret to mean that the total fluorescence signal obtained from ANS increases as the proteins increase in saturation state and approach a meta-stable state.

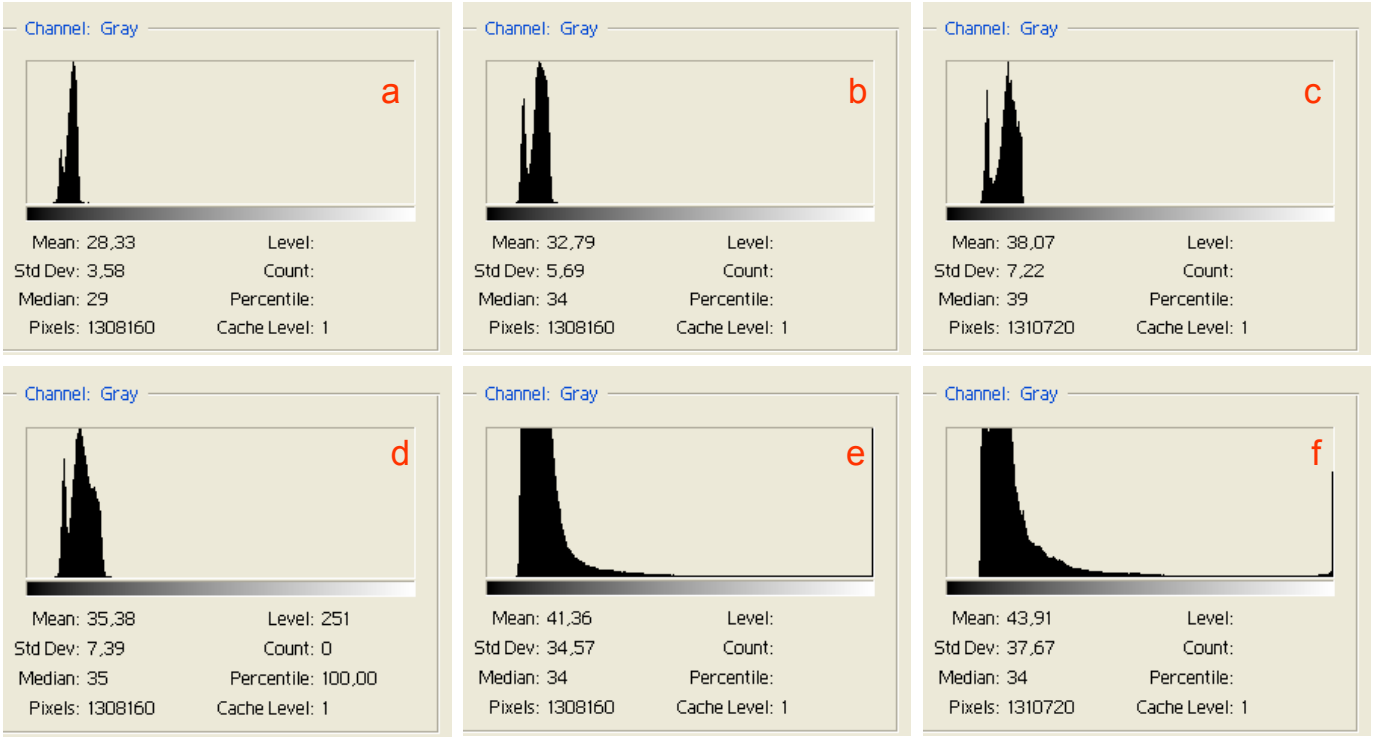

Fig. 17.Intensity Histograms of the crystallization images presented in Fig. 16.

This correlated change in the intensity histograms prompted us to manually change the grey scale used to display the images. Rather than the full range of 0-256 being used to represent the black-white gradient a new scale of 30-50 for black-white was applied to each image. The results of this rescaling are presented in Fig. 18 below. While the intensity histograms provide very much the same data an analysis of these images

allowed the spatial distribution of the intensities to be determined. While the dye and protein concentrations remain identical in each image there is a marked variation in the low intensity fluorescence produced.

Examination of 18a and b demonstrates an evenly distributed increase in fluorescence throughout the drop. The image presented in 18c shows a further increase in fluorescence signal intensity, but additionally shows some spatial distribution of the obtained signal. This distribution is not visible in figure 16c. As the precipitation concentration further increases (Fig. 18d) a strong in-homogeneity is observed along with a stronger fluorescence signal. Distinct regions of Fig. 18d now start to show a punctuate nature, which would be consistent with light precipitation phenomena classically observed in crystallization experiments. However, direct comparison with Fig 16d reveals that no such punctuate precipitate is seen under visible light conditions. This suggests that the increased fluorescence signals are due to the formation of critical nuclei (cf Fig. 2).

The application of this increased contrast results in many saturated pixels in images 18e and 18f – due to the greatly increased fluorescent signal produced by the formation of protein crystals. However, examination of the non-saturated regions of the image clearly shows the presence of punctuate regions of the crystallization experiment which show significant fluorescence. Comparison with Figs. 16e and 16f again demonstrates that no punctuate precipitate is visible under standard visible illumination conditions. The potential use of this will be discussed below in Section 4.

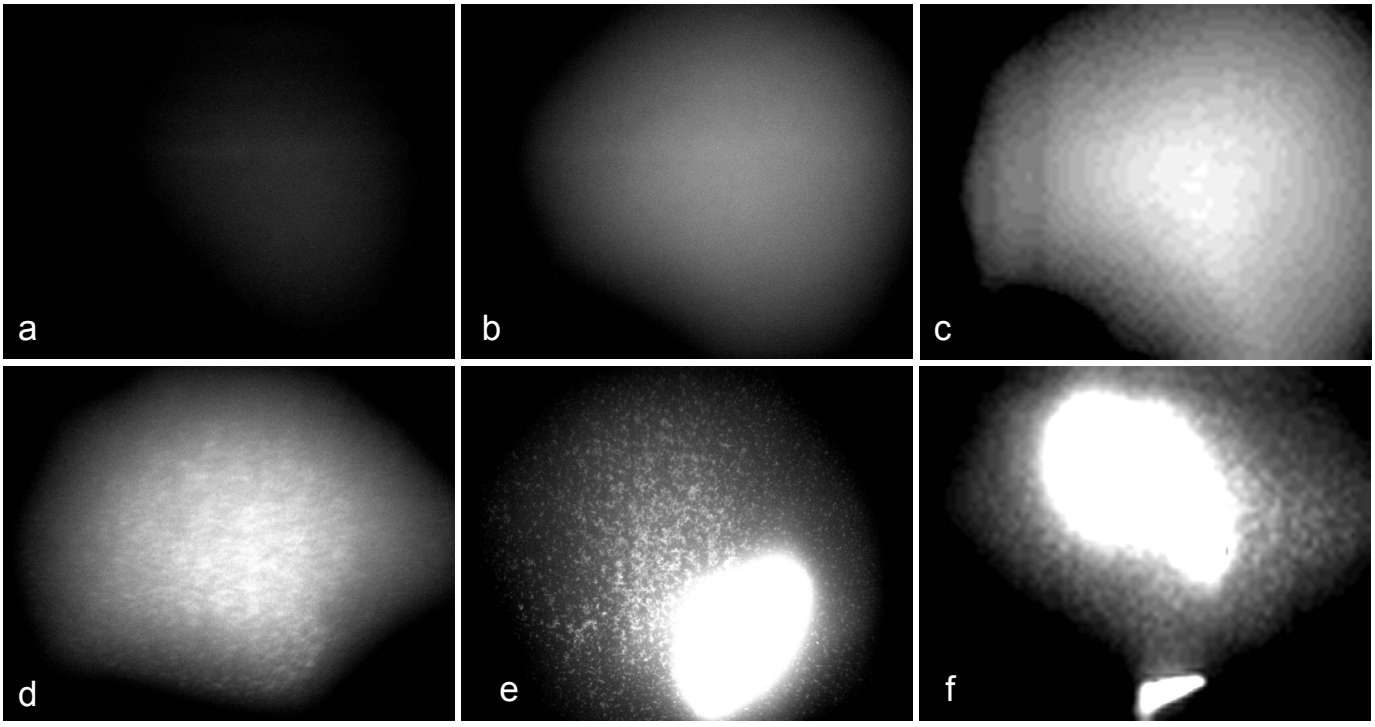

Fig. 18 Rescaled fluorescence images of lysozyme crystallization trials..

4 Discussion

It should be stressed at this point that only an initial analysis has been performed and that significant further work is required. However, our initial results are highly encouraging. The images presented above clearly demonstrate that the addition of a non-invasive probe (ANS) to the crystallization experiments provides significant additional information upon the solution state of the sample under investigation. The absolute fluorescence signal (intensity histogram) increases as the protein reaches the meta-stable region of the phase diagram. This effect can be exploited in the classification of crystallization experiments, even in the absence of crystals. Indeed, we show above that ranking of the images is possible under fluorescent conditions when under visible light conditions no significant differences can be observed.

We interpret the punctuate distribution fluorescent signal as an indication that the protein in solution is reaching a state under which critical nuclei can form. Visible light illumination again shows no such formations. This would be the first direct detection of critical nuclei within a crystallization experiment. Previous experiments have been performed which demonstrate the existence of such nuclei (REF Naomi Chayenne), but these experiments have relied on biophysical manipulation of the sample (filtration/static/dynamic light scattering/etc.). The method described above would require so such additional handling – other than a change in the illumination conditions used for drop imaging.

Acknowledgements

I would like to thank DESY Summer School organizing committee and EMBL Outstation Hamburg for help and support. My special thanks to my supervisor Dr. Matthew Groves,

for providing me with information and basic knowledge about the protein crystallography. Also many thanks to our collegues Dr. Rositsa Jordanova, Dr. Ingrid Birgit Mueller, Dr. Xandra Kreplin for they support and stimulating discussions.

Supplementary Information

GT1.xls

Tray Location	Reagent number	[Salt]	[Salt]_units	Salt	[Buffer]	[Buffer]_units	Buffer	pH	[Precip1]	[Precip1]_units
A1	ANSLYS_1	0,20	M	ammonium sulfate	0,10	M	sodium acetate pH 4.6	4,6	0,00	%w/v
A2	ANSLYS_2	0,20	M	ammonium sulfate	0,10	M	sodium acetate pH 4.6	4,6	3,00	%w/v
A3	ANSLYS_3	0,20	M	ammonium sulfate	0,10	M	sodium acetate pH 4.6	4,6	6,00	%w/v
A4	ANSLYS_4	0,20	M	ammonium sulfate	0,10	M	sodium acetate pH 4.6	4,6	9,00	%w/v
A5	ANSLYS_5	0,20	M	ammonium sulfate	0,10	M	sodium acetate pH 4.6	4,6	12,00	%w/v
A6	ANSLYS_6	0,20	M	ammonium sulfate	0,10	M	sodium acetate pH 4.6	4,6	15,00	%w/v
A7	ANSLYS_7	0,20	M	ammonium sulfate	0,10	M	sodium acetate pH 4.6	4,6	18,00	%w/v
A8	ANSLYS_8	0,20	M	ammonium sulfate	0,10	M	sodium acetate pH 4.6	4,6	21,00	%w/v
A9	ANSLYS_9	0,20	M	ammonium sulfate	0,10	M	sodium acetate pH 4.6	4,6	24,00	%w/v
A10	ANSLYS_10	0,20	M	ammonium sulfate	0,10	M	sodium acetate pH 4.6	4,6	27,00	%w/v
A11	ANSLYS_11	0,20	M	ammonium sulfate	0,10	M	sodium acetate pH 4.6	4,6	30,00	%w/v
A12	ANSLYS_12	0,20	M	ammonium sulfate	0,10	M	sodium acetate pH 4.6	4,6	33,00	%w/v
B1	ANSLYS_13				0,10	M	sodium acetate pH 4.6	4,6	0,00	%w/v
B2	ANSLYS_14				0,10	M	sodium acetate pH 4.6	4,6	3,00	%w/v
B3	ANSLYS_15				0,10	M	sodium acetate pH 4.6	4,6	6,00	%w/v
B4	ANSLYS_16				0,10	M	sodium acetate pH 4.6	4,6	9,00	%w/v
B5	ANSLYS_17				0,10	M	sodium acetate pH 4.6	4,6	12,00	%w/v
B6	ANSLYS_18				0,10	M	sodium acetate pH 4.6	4,6	15,00	%w/v
B7	ANSLYS_19				0,10	M	sodium acetate pH 4.6	4,6	18,00	%w/v
B8	ANSLYS_20				0,10	M	sodium acetate pH 4.6	4,6	21,00	%w/v
B9	ANSLYS_21				0,10	M	sodium acetate pH 4.6	4,6	24,00	%w/v
B10	ANSLYS_22				0,10	M	sodium acetate pH 4.6	4,6	27,00	%w/v
B11	ANSLYS_23				0,10	M	sodium acetate pH 4.6	4,6	30,00	%w/v
B12	ANSLYS_24				0,10	M	sodium acetate pH 4.6	4,6	33,00	%w/v
C1	ANSLYS_25	0,20	M	ammonium sulfate	0,10	M	sodium acetate pH 3.0	3,0	25,00	%w/v
C2	ANSLYS_26	0,20	M	ammonium sulfate	0,10	M	sodium acetate pH 3.5	3,5	25,00	%w/v
C3	ANSLYS_27	0,20	M	ammonium sulfate	0,10	M	sodium acetate pH 4.0	4,0	25,00	%w/v
C4	ANSLYS_28	0,20	M	ammonium sulfate	0,10	M	sodium acetate pH 4.5	4,5	25,00	%w/v
C5	ANSLYS_29	0,20	M	ammonium sulfate	0,10	M	sodium acetate pH 5.0	5,0	25,00	%w/v
C6	ANSLYS_30	0,20	M	ammonium sulfate	0,10	M	sodium acetate pH 5.5	5,5	25,00	%w/v
C7	ANSLYS_31	0,20	M	ammonium sulfate	0,10	M	sodium acetate pH 6.0	6,0	25,00	%w/v
C8	ANSLYS_32	0,20	M	ammonium sulfate	0,10	M	sodium acetate pH 6.5	6,5	25,00	%w/v
C9	ANSLYS_33	0,20	M	ammonium sulfate	0,10	M	sodium acetate pH 7.0	7,0	25,00	%w/v
C10	ANSLYS_34	0,20	M	ammonium sulfate	0,10	M	sodium acetate pH 7.5	7,5	25,00	%w/v
C11	ANSLYS_35	0,20	M	ammonium sulfate	0,10	M	sodium acetate pH 8.0	8,0	25,00	%w/v
C12	ANSLYS_36	0,20	M	ammonium sulfate	0,10	M	sodium acetate pH 8.5	8,5	25,00	%w/v
D1	ANSLYS_37				0,10	M	sodium acetate pH 3.0	3,0	25,00	%w/v
D2	ANSLYS_38				0,10	M	sodium acetate pH 3.5	3,5	25,00	%w/v
D3	ANSLYS_39				0,10	M	sodium acetate pH 4.0	4,0	25,00	%w/v
D4	ANSLYS_40				0,10	M	sodium acetate pH 4.5	4,5	25,00	%w/v
D5	ANSLYS_41				0,10	M	sodium acetate pH 5.0	5,0	25,00	%w/v
D6	ANSLYS_42				0,10	M	sodium acetate pH 5.5	5,5	25,00	%w/v
D7	ANSLYS_43				0,10	M	sodium acetate pH 6.0	6,0	25,00	%w/v
D8	ANSLYS_44				0,10	M	sodium acetate pH 6.5	6,5	25,00	%w/v
D9	ANSLYS_45				0,10	M	sodium acetate pH 7.0	7,0	25,00	%w/v
D10	ANSLYS_46				0,10	M	sodium acetate pH 7.5	7,5	25,00	%w/v
D11	ANSLYS_47				0,10	M	sodium acetate pH 8.0	8,0	25,00	%w/v
D12	ANSLYS_48				0,10	M	sodium acetate pH 8.5	8,5	25,00	%w/v
E1	ANSLYS_49	0,20	M	calcium chloride	0,10	M	sodium acetate pH 4.6	4,6	0,00	%v/v
E2	ANSLYS_50	0,20	M	calcium chloride	0,10	M	sodium acetate pH 4.6	4,6	3,00	%v/v
E3	ANSLYS_51	0,20	M	calcium chloride	0,10	M	sodium acetate pH 4.6	4,6	6,00	%v/v
E4	ANSLYS_52	0,20	M	calcium chloride	0,10	M	sodium acetate pH 4.6	4,6	9,00	%v/v
E5	ANSLYS_53	0,20	M	calcium chloride	0,10	M	sodium acetate pH 4.6	4,6	12,00	%v/v
E6	ANSLYS_54	0,20	M	calcium chloride	0,10	M	sodium acetate pH 4.6	4,6	15,00	%v/v
E7	ANSLYS_55	0,20	M	calcium chloride	0,10	M	sodium acetate pH 4.6	4,6	18,00	%v/v
E8	ANSLYS_56	0,20	M	calcium chloride	0,10	M	sodium acetate pH 4.6	4,6	21,00	%v/v
E9	ANSLYS_57	0,20	M	calcium chloride	0,10	M	sodium acetate pH 4.6	4,6	24,00	%v/v
E10	ANSLYS_58	0,20	M	calcium chloride	0,10	M	sodium acetate pH 4.6	4,6	27,00	%v/v
E11	ANSLYS_59	0,20	M	calcium chloride	0,10	M	sodium acetate pH 4.6	4,6	30,00	%v/v
E12	ANSLYS_60	0,20	M	calcium chloride	0,10	M	sodium acetate pH 4.6	4,6	33,00	%v/v
F1	ANSLYS_61				0,10	M	sodium acetate pH 4.6	4,6	0,00	%v/v
F2	ANSLYS_62				0,10	M	sodium acetate pH 4.6	4,6	3,00	%v/v
F3	ANSLYS_63				0,10	M	sodium acetate pH 4.6	4,6	6,00	%v/v
F4	ANSLYS_64				0,10	M	sodium acetate pH 4.6	4,6	9,00	%v/v
F5	ANSLYS_65				0,10	M	sodium acetate pH 4.6	4,6	12,00	%v/v
F6	ANSLYS_66				0,10	M	sodium acetate pH 4.6	4,6	15,00	%v/v
F7	ANSLYS_67				0,10	M	sodium acetate pH 4.6	4,6	18,00	%v/v
F8	ANSLYS_68				0,10	M	sodium acetate pH 4.6	4,6	21,00	%v/v
F9	ANSLYS_69				0,10	M	sodium acetate pH 4.6	4,6	24,00	%v/v
F10	ANSLYS_70				0,10	M	sodium acetate pH 4.6	4,6	27,00	%v/v
F11	ANSLYS_71				0,10	M	sodium acetate pH 4.6	4,6	30,00	%v/v
F12	ANSLYS_72				0,10	M	sodium acetate pH 4.6	4,6	33,00	%v/v

GT2.xls

Tray Location	Reagent number	[Salt]	[Salt]_units	Salt	[Buffer]	[Buffer]_units	Buffer	pH	[Precip1]	[Precip1]_units
A1	ANS2LYS_1				0,10	M	sodium acetate pH 4.6	4,6	0,00	M
A2	ANS2LYS_2				0,10	M	sodium acetate pH 4.6	4,6	0,20	M
A3	ANS2LYS_3				0,10	M	sodium acetate pH 4.6	4,6	0,40	M
A4	ANS2LYS_4				0,10	M	sodium acetate pH 4.6	4,6	0,60	M
A5	ANS2LYS_5				0,10	M	sodium acetate pH 4.6	4,6	0,80	M
A6	ANS2LYS_6				0,10	M	sodium acetate pH 4.6	4,6	1,00	M
A7	ANS2LYS_7				0,10	M	sodium acetate pH 4.6	4,6	1,20	M
A8	ANS2LYS_8				0,10	M	sodium acetate pH 4.6	4,6	1,40	M
A9	ANS2LYS_9				0,10	M	sodium acetate pH 4.6	4,6	1,60	M
A10	ANS2LYS_10				0,10	M	sodium acetate pH 4.6	4,6	1,80	M
A11	ANS2LYS_11				0,10	M	sodium acetate pH 4.6	4,6	2,00	M
A12	ANS2LYS_12				0,10	M	sodium acetate pH 4.6	4,6	2,20	M
B1	ANS2LYS_13				0,10	M	sodium acetate pH 3.0	3,0	2,00	M
B2	ANS2LYS_14				0,10	M	sodium acetate pH 3.5	3,5	2,00	M
B3	ANS2LYS_15				0,10	M	sodium acetate pH 4.0	4,0	2,00	M
B4	ANS2LYS_16				0,10	M	sodium acetate pH 4.5	4,5	2,00	M
B5	ANS2LYS_17				0,10	M	sodium acetate pH 5.0	5,0	2,00	M
B6	ANS2LYS_18				0,10	M	sodium acetate pH 5.5	5,5	2,00	M
B7	ANS2LYS_19				0,10	M	sodium acetate pH 6.0	6,0	2,00	M
B8	ANS2LYS_20				0,10	M	sodium acetate pH 6.5	6,5	2,00	M
B9	ANS2LYS_21				0,10	M	sodium acetate pH 7.0	7,0	2,00	M
B10	ANS2LYS_22				0,10	M	sodium acetate pH 7.5	7,5	2,00	M
B11	ANS2LYS_23				0,10	M	sodium acetate pH 8.0	8,0	2,00	M
B12	ANS2LYS_24				0,10	M	sodium acetate pH 8.5	8,5	2,00	M
C1	ANS2LYS_25								0,00	M
C2	ANS2LYS_26								0,20	M
C3	ANS2LYS_27								0,40	M
C4	ANS2LYS_28								0,60	M
C5	ANS2LYS_29								0,80	M
C6	ANS2LYS_30								1,00	M
C7	ANS2LYS_31								1,20	M
C8	ANS2LYS_32								1,40	M
C9	ANS2LYS_33								1,60	M
C10	ANS2LYS_34								1,80	M
C11	ANS2LYS_35								2,00	M
C12	ANS2LYS_36								2,20	M
D1	ANS2LYS_37				0,10	M	sodium acetate pH 3.0	3,0	2,00	M
D2	ANS2LYS_38				0,10	M	sodium acetate pH 3.5	3,5	2,00	M
D3	ANS2LYS_39				0,10	M	sodium acetate pH 4.0	4,0	2,00	M
D4	ANS2LYS_40				0,10	M	sodium acetate pH 4.5	4,5	2,00	M
D5	ANS2LYS_41				0,10	M	sodium acetate pH 5.0	5,0	2,00	M
D6	ANS2LYS_42				0,10	M	sodium acetate pH 5.5	5,5	2,00	M
D7	ANS2LYS_43				0,10	M	sodium acetate pH 6.0	6,0	2,00	M
D8	ANS2LYS_44				0,10	M	sodium acetate pH 6.5	6,5	2,00	M
D9	ANS2LYS_45				0,10	M	sodium acetate pH 7.0	7,0	2,00	M
D10	ANS2LYS_46				0,10	M	sodium acetate pH 7.5	7,5	2,00	M
D11	ANS2LYS_47				0,10	M	sodium acetate pH 8.0	8,0	2,00	M
D12	ANS2LYS_48				0,10	M	sodium acetate pH 8.5	8,5	2,00	M
E1	ANS2LYS_49								0,00	%v/v
E2	ANS2LYS_50								3,00	%v/v
E3	ANS2LYS_51								6,00	%v/v
E4	ANS2LYS_52								9,00	%v/v
E5	ANS2LYS_53								12,00	%v/v
E6	ANS2LYS_54								15,00	%v/v
E7	ANS2LYS_55								18,00	%v/v
E8	ANS2LYS_56								21,00	%v/v
E9	ANS2LYS_57								24,00	%v/v
E10	ANS2LYS_58								27,00	%v/v
E11	ANS2LYS_59								30,00	%v/v
E12	ANS2LYS_60								33,00	%v/v
F1	ANS2LYS_61				0,10	M	sodium acetate pH 3.0	3,0	25,00	%v/v
F2	ANS2LYS_62				0,10	M	sodium acetate pH 3.5	3,5	25,00	%v/v
F3	ANS2LYS_63				0,10	M	sodium acetate pH 4.0	4,0	25,00	%v/v
F4	ANS2LYS_64				0,10	M	sodium acetate pH 4.5	4,5	25,00	%v/v
F5	ANS2LYS_65				0,10	M	sodium acetate pH 5.0	5,0	25,00	%v/v
F6	ANS2LYS_66				0,10	M	sodium acetate pH 5.5	5,5	25,00	%v/v
F7	ANS2LYS_67				0,10	M	sodium acetate pH 6.0	6,0	25,00	%v/v
F8	ANS2LYS_68				0,10	M	sodium acetate pH 6.5	6,5	25,00	%v/v
F9	ANS2LYS_69				0,10	M	sodium acetate pH 7.0	7,0	25,00	%v/v
F10	ANS2LYS_70				0,10	M	sodium acetate pH 7.5	7,5	25,00	%v/v
F11	ANS2LYS_71				0,10	M	sodium acetate pH 8.0	8,0	25,00	%v/v
F12	ANS2LYS_72				0,10	M	sodium acetate pH 8.5	8,5	25,00	%v/v

GT3.xls

Tray Location	Reagent number	[Salt]	[Salt]_units	Salt	[Buffer]	[Buffer]_units	Buffer	pH	[Precip1]	[Precip1]_units
A1	ANSLYS-Neg_1				0,10	M	HEPES pH 7.5	7,5	45,00	%v/v
A2	ANSLYS-Neg_2				0,10	M	HEPES pH 7.5	7,5	0,00	%v/v
A3	ANSLYS-Neg_3				0,10	M	HEPES pH 7.5	7,5	0,20	M
A4	ANSLYS-Neg_4				0,10	M	Tris pH 8.5	8,5	0,00	%v/v
A5	ANSLYS-Neg_5				3,00	M	sodium formate pH 6.0	6,0		
A6	ANSLYS-Neg_6				3,00	M	sodium formate pH 6.5	6,5		
A7	ANSLYS-Neg_7				3,00	M	sodium formate pH 7.0	7,0		
A8	ANSLYS-Neg_8				3,00	M	sodium formate pH 8.5	8,5		
A9	ANSLYS-Neg_9				1,00	M	sodium malonate pH 4.0	4,0		
A10	ANSLYS-Neg_10				1,00	M	sodium malonate pH 5.0	5,0		
A11	ANSLYS-Neg_11				1,00	M	sodium malonate pH 6.0	6,0		
A12	ANSLYS-Neg_12				1,00	M	sodium malonate pH 7.0	7,0		
B1	ANSLYS-Neg_13				0,10	M	HEPES pH 7.5	7,5	50,00	%v/v
B2	ANSLYS-Neg_14				0,10	M	HEPES pH 7.5	7,5	4,00	%v/v
B3	ANSLYS-Neg_15				0,10	M	HEPES pH 7.5	7,5	0,30	M
B4	ANSLYS-Neg_16				0,10	M	Tris pH 8.5	8,5	4,00	%v/v
B5	ANSLYS-Neg_17				3,50	M	sodium formate pH 6.0	6,0		
B6	ANSLYS-Neg_18				3,50	M	sodium formate pH 6.5	6,5		
B7	ANSLYS-Neg_19				3,50	M	sodium formate pH 7.0	7,0		
B8	ANSLYS-Neg_20				3,50	M	sodium formate pH 8.5	8,5		
B9	ANSLYS-Neg_21				1,40	M	sodium malonate pH 4.0	4,0		
B10	ANSLYS-Neg_22				1,40	M	sodium malonate pH 5.0	5,0		
B11	ANSLYS-Neg_23				1,40	M	sodium malonate pH 6.0	6,0		
B12	ANSLYS-Neg_24				1,40	M	sodium malonate pH 7.0	7,0		
C1	ANSLYS-Neg_25				0,10	M	HEPES pH 7.5	7,5	55,00	%v/v
C2	ANSLYS-Neg_26				0,10	M	HEPES pH 7.5	7,5	8,00	%v/v
C3	ANSLYS-Neg_27				0,10	M	HEPES pH 7.5	7,5	0,40	M
C4	ANSLYS-Neg_28				0,10	M	Tris pH 8.5	8,5	8,00	%v/v
C5	ANSLYS-Neg_29				4,00	M	sodium formate pH 6.0	6,0		
C6	ANSLYS-Neg_30				4,00	M	sodium formate pH 6.5	6,5		
C7	ANSLYS-Neg_31				4,00	M	sodium formate pH 7.0	7,0		
C8	ANSLYS-Neg_32				4,00	M	sodium formate pH 8.5	8,5		
C9	ANSLYS-Neg_33				1,80	M	sodium malonate pH 4.0	4,0		
C10	ANSLYS-Neg_34				1,80	M	sodium malonate pH 5.0	5,0		
C11	ANSLYS-Neg_35				1,80	M	sodium malonate pH 6.0	6,0		
C12	ANSLYS-Neg_36				1,80	M	sodium malonate pH 7.0	7,0		
D1	ANSLYS-Neg_37				0,10	M	HEPES pH 7.5	7,5	60,00	%v/v
D2	ANSLYS-Neg_38				0,10	M	HEPES pH 7.5	7,5	12,00	%v/v
D3	ANSLYS-Neg_39				0,10	M	HEPES pH 7.5	7,5	0,50	M
D4	ANSLYS-Neg_40				0,10	M	Tris pH 8.5	8,5	12,00	%v/v
D5	ANSLYS-Neg_41				4,50	M	sodium formate pH 6.0	6,0		
D6	ANSLYS-Neg_42				4,50	M	sodium formate pH 6.5	6,5		
D7	ANSLYS-Neg_43				4,50	M	sodium formate pH 7.0	7,0		
D8	ANSLYS-Neg_44				4,50	M	sodium formate pH 8.5	8,5		
D9	ANSLYS-Neg_45				2,20	M	sodium malonate pH 4.0	4,0		
D10	ANSLYS-Neg_46				2,20	M	sodium malonate pH 5.0	5,0		
D11	ANSLYS-Neg_47				2,20	M	sodium malonate pH 6.0	6,0		
D12	ANSLYS-Neg_48				2,20	M	sodium malonate pH 7.0	7,0		
E1	ANSLYS-Neg_49				0,10	M	HEPES pH 7.5	7,5	65,00	%v/v
E2	ANSLYS-Neg_50				0,10	M	HEPES pH 7.5	7,5	16,00	%v/v
E3	ANSLYS-Neg_51				0,10	M	HEPES pH 7.5	7,5	0,60	M
E4	ANSLYS-Neg_52				0,10	M	Tris pH 8.5	8,5	16,00	%v/v
E5	ANSLYS-Neg_53				5,00	M	sodium formate pH 6.0	6,0		
E6	ANSLYS-Neg_54				5,00	M	sodium formate pH 6.5	6,5		
E7	ANSLYS-Neg_55				5,00	M	sodium formate pH 7.0	7,0		
E8	ANSLYS-Neg_56				5,00	M	sodium formate pH 8.5	8,5		
E9	ANSLYS-Neg_57				2,60	M	sodium malonate pH 4.0	4,0		
E10	ANSLYS-Neg_58				2,60	M	sodium malonate pH 5.0	5,0		
E11	ANSLYS-Neg_59				2,60	M	sodium malonate pH 6.0	6,0		
E12	ANSLYS-Neg_60				2,60	M	sodium malonate pH 7.0	7,0		
F1	ANSLYS-Neg_61				0,10	M	HEPES pH 7.5	7,5	70,00	%v/v
F2	ANSLYS-Neg_62				0,10	M	HEPES pH 7.5	7,5	20,00	%v/v
F3	ANSLYS-Neg_63				0,10	M	HEPES pH 7.5	7,5	0,70	M
F4	ANSLYS-Neg_64				0,10	M	Tris pH 8.5	8,5	20,00	%v/v
F5	ANSLYS-Neg_65				5,50	M	sodium formate pH 6.0	6,0		
F6	ANSLYS-Neg_66				5,50	M	sodium formate pH 6.5	6,5		
F7	ANSLYS-Neg_67				5,50	M	sodium formate pH 7.0	7,0		
F8	ANSLYS-Neg_68				5,50	M	sodium formate pH 8.5	8,5		
F9	ANSLYS-Neg_69				3,00	M	sodium malonate pH 4.0	4,0		
F10	ANSLYS-Neg_70				3,00	M	sodium malonate pH 5.0	5,0		
F11	ANSLYS-Neg_71				3,00	M	sodium malonate pH 6.0	6,0		
F12	ANSLYS-Neg_72				3,00	M	sodium malonate pH 7.0	7,0		